Reproductive Toxicology 55 (2015) 20–29

Contents lists available at ScienceDirect

Reproductive Toxicology

journal homepage: www.elsevier.com/locate/reprotox

Identification of environmental chemicals that induce yolk malabsorption in zebrafish using automated image segmentation

Sharanya Maanasi Kalasekar[a,1], Eleni Zacharia[b,1], Noah Kessler[b], Nicole A. Ducharme[a], Jan-Åke Gustafsson[a,c], Ioannis A. Kakadiaris[b], Maria Bondesson[a,*]

[a] Center for Nuclear Receptors and Cell Signaling, Department of Biology and Biochemistry, University of Houston, Houston, TX 77204, USA
[b] Department of Computer Science, University of Houston, Houston, TX 77204, USA
[c] Karolinska Institutet, Department of Biosciences and Nutrition, 14183 Huddinge, Sweden

ARTICLE INFO

Article history:
Received 20 May 2014
Received in revised form 16 October 2014
Accepted 17 October 2014
Available online 5 November 2014

Keywords:
Zebrafish
Yolk
Toxicity
Image analysis
High throughput screening

ABSTRACT

Environmental factors affecting nutrient availability during development can cause predisposition to diseases later in life. To identify chemicals in the environment capable of altering nutrient mobilization, we analyzed yolk malabsorption in the zebrafish embryo, which relies on maternally-derived yolk for nutrition during its first week of life. Embryos of the transgenic zebrafish line HGn50D, which fluoresce in the yolk syncytial layer, were exposed from two to five days post fertilization to different chemicals. We developed a software package to automatically and accurately segment and quantify the area of the fluorescing yolk in images captured at the end of the treatment period. Based on this quantification, we found that prochloraz decreased yolk absorption, while butralin, tetrabromobisphenol A, tetrachlorobisphenol A and tributyltin increased yolk absorption. Given the number and variety of industrial chemicals in commerce today, development of automated image processing to perform high-speed quantitative analysis of biological effects is an important step for enabling high throughput screening to identify chemicals altering nutrient absorption.

1. Introduction

Availability of nutrients is one of the major factors determining embryonic growth and development. Optimal nutrition is essential for embryo survival and organogenesis (reviewed in [1]). Insufficient or excess nutrition during intrauterine development is known to cause permanent endocrine and metabolic changes: these perturbations leave "imprints", which can manifest later in life as diseases, such as obesity, diabetes, or hypertension (reviewed in [2]).

Environmental factors (e.g., exposure to industrial chemicals) affecting the nutritional status of the developing embryo can alter its homeostatic processes and induce disease. Studies investigating the role of nutrient–toxicant interactions in disease etiology have often focused on the effect of nutrition in modulating chemical toxicity (reviewed in [3–5]). Studying the effects of environmental chemicals on nutrient availability and mobilization may be equally important to improving our understanding of nutrient–toxicant interplay, particularly during development.

Zebrafish (*Danio rerio*) is a suitable model for studies of nutrient mobilization during development. Like other oviparous species, the zebrafish embryo carries its own yolk to provide energy and nutrients during the early developmental phase. The teleost yolk is composed predominantly of phospholipids and triacylglycerols packed into lipoprotein particles (reviewed in [6]). From zygote formation to about 5 days post fertilization (dpf), the developing zebrafish embryo (larva, after hatching at 2–3 dpf) derives its energy from endogenous yolk metabolism. This marks the endotrophic stage of development. By 5 dpf, a functional gut has formed [7] and the larvae can begin ingesting food while still deriving energy from the yolk. Once the yolk is completely depleted, the larva enters an exotrophic nutrition mode, relying on exogenous, ingested food for energy [8]. In the embryo, the yolk is surrounded by the yolk syncytial layer, an extra-embryonic tissue formed during the blastula stage (reviewed in [9]). One of the yolk syncytial

* Corresponding author at: University of Houston, Center for Nuclear Receptors and Cell Signaling, 3605 Cullen Blvd, Science and Engineering Research Center Bldg 545, Houston, TX 77204-5056, USA. Tel.: +1 832 842 8805; fax: +1 713 743 0634.
E-mail address: mbondessonbolin@uh.edu (M. Bondesson).
[1] These authors contributed equally to the work.

http://dx.doi.org/10.1016/j.reprotox.2014.10.022
0890-6238/

layer's functions throughout early embryonic development is to hydrolyze yolk materials and transport them from the yolk to the embryonic cells and larval tissues. In addition, it plays important roles during development including controlling embryo patterning and morphogenesis (reviewed in [9]). The yolk syncytial layer is a syncytium containing many yolk syncytial nuclei, which have high transcriptional activity of genes involved in early metabolism, such as steroidogenesis, iron transport, and lipid metabolism [10–12].

Lack of nutrients during development may lead to embryonic malabsorption syndrome in zebrafish characterized by small body size and large yolk. For example, knock-down of the microsomal triglyceride transfer protein (Mtp), a protein involved in lipid transport and normally expressed in the yolk syncytial layer of the zebrafish embryo, results in decreased yolk consumption and loss of lipid staining of the embryo in other locations than of the yolk [13]. In addition, the Mtp knock-down embryos are small and die by 6 dpf with pronounced edema. Exposure to certain drugs or environmental chemicals has also been shown to induce malabsorption. For example, both cholesterol lowering drugs and the pesticide prochloraz decrease yolk absorption [14,15]. Potentially, many more chemicals could induce embryonic malabsorption syndrome, but due to the lack of high throughput assays for yolk absorption, few chemicals have been investigated for this effect. In the present study, we describe the development of a screening model to examine nine chemicals' effect on zebrafish yolk uptake. The model is based on the transgenic zebrafish (HGn50D) expressing the Green Fluorescent Protein (GFP) in the yolk syncytial layer. We developed a software package named ZebRA to automatically and accurately segment and quantify the yolk in HGn50D embryos imaged by fluorescent microscopy. Given the number and variety of industrial chemicals in commerce today, the development of an automated software package for the segmentation and quantification of biological effects is an important step for enabling high throughput screening to identify adversely acting chemicals because: (i) it will allow fast performance, (ii) it will allow accurate quantification of biological effects and (iii) it will enhance reliability and reproducibility of the experiments. Using our software package, the yolk size was examined in embryos that had been exposed to chemicals from 2 dpf, when morphogenesis of organ rudiments is almost complete [16], to 5 dpf, when the endotrophic period ends. Our method of automated image analysis will allow for future high throughput screening for developmental toxicants causing yolk malabsorption.

2. Materials and methods

2.1. Zebrafish maintenance

Transgenic fish HGn50D were obtained from Dr. Kawakami, the National BioResource Project from the Ministry of Education, Culture, Sports, Science and Technology of Japan [17,18]. HGN50D and wildtype TAB14 zebrafish were housed and used according to the maintenance and experimental protocols approved by the Institutional Animal Care and Use Committee at University of Houston. Adult zebrafish were maintained in 3.5 L tanks in a Tecniplast system (Tecniplast USA Inc., West Chester, PA) supplied continuously with circulating filtered water at 28.5 °C on a 14 h/10 h light/dark cycle.

2.2. Chemicals

Prochloraz (purity 99.1%, CAS 67747-09-5), tributyltin (TBT) chloride (96%, CAS 1461-22-9), tetrabromobisphenol A (TBBPA, 2,2-bis(3,5-dibromo-4-hydroxyphenyl)propane) (97%, CAS 79-94-7), perfluorooctanoic acid (PFOA) (96%, CAS 335-67-1), imazalil (99.7%, CAS 35554-44-0), butralin (99.8%, CAS 33629-47-9), clofibrate (CAS 637-07-0), and gemfibrozil (CAS 25812-30-0) were obtained from Sigma–Aldrich (St. Louis, MO). Tetrachlorobisphenol A (TCBPA, 2,2-bis(3,5-dichloro-4-hydroxyphenyl)propane) (95%, CAS 79-95-8) was purchased from TCI America (Portland, OR). All chemicals were dissolved and diluted in DMSO to make 1000X stock solutions.

2.3. Oil Red O Staining

Embryos were harvested after spawning and housed in a 28.5 °C incubator with 14 h/10 h light/dark cycle in embryo media E3 (5 mM NaCl, 0.17 mM KCl, 0.33 mM $CaCl_2$, and 0.33 mM $MgSO_4$). At 2 and 5 dpf, larvae were euthanized in tricaine methylsulfonate (MS-222, Sigma–Aldrich), and fixed in 4% paraformaldehyde overnight at 4 °C. Fixed larvae were then washed with 0.1% Tween-20 in PBS (PBT), and stained with a 0.3% Oil Red O (ORO) solution for 3 h at room temperature. Staining was followed by PBT washes. Stained larvae were then stored in 90% glycerol.

2.4. Embryo treatment and imaging

HGn50D embryos were harvested after spawning and allowed to develop in a Petri dish at 28.5 °C with 14 h/10 h light/dark cycle in E3 media. At 2 dpf, a clutch of 20 embryos were transferred into each well of a 6-well plate containing 4 mL E3. The embryos were exposed to compounds dissolved in dimethylsulfoxide (DMSO) or to DMSO alone (vehicle-control). At 5 dpf, the larvae were transferred to 96-well plates (1 embryo/well in approximately 100 μL E3), manually imaged on an Olympus IX51 inverted fluorescence microscope using a 4× objective, and images captured using an Olympus XM10 camera with CellSens Dimension v1.9 software (Olympus). Exposures were not performed directly in 96 well plates because the small volume could result in motility restriction, thereby causing decreased yolk absorption. The larvae were not anaesthetized, and thus swam in an upright position, facilitating image capture of the ventral side of the larvae. Chemical exposure experiments for all concentrations were repeated 2–4 times, with 1–2 sets of 20 embryos per experiment. Images of ORO stained zebrafish were acquired using a Nikon AZ100 M microscope with a color camera DS Fi1 (Nikon) and the NIS-Elements AR analyzing program. For confocal imaging, embryos were imaged at 72 hpf using an Olympus FluoView 1000 confocal microscope with an 800 × 800 aspect ratio at 4 μs/pixel using the default eGFP filter setting. Images were processed by Olympus Fluoview software.

To determine LC_{50} values and morphological malformations, a clutch of 20 TAB 14 embryos were exposed to a dose range of the compounds at 2 dpf, and lethality and morphology were scored at 5 dpf.

Dissolved oxygen measurements were made using a Milwaukee AQ600 Portable Oxygen Meter. E3 from three wells was pooled to yield 12 mL of sample for the measurements.

Most of the chemicals in this study have previously been shown to be stable in aquatic solutions. The reported half-lives of the compounds are 22.6 days for prochloraz [19], between 6 days and 35 weeks for tributyltin (search term "tributyltin" at https://pubchem.ncbi.nlm.nih.gov), at least 8 weeks for imazalil [20], 21–52 days for butralin (search term "butralin" at https://pubchem.ncbi.nlm.nih.gov), and years rather than days for PFOA [21]. However, the experimental setups for these measurements may differ from the experimental conditions used here, and, thus, there might be factors, such as chemical binding to plastic surfaces, which could alter the actual chemical exposure

concentrations used here. We have previously shown under similar experimental conditions as used here that TBBPA and TCBPA are rapidly taken up and metabolized by zebrafish larvae [22]. A linear range uptake following exposure to increasing doses of clofibrate and gemfibrozil in zebrafish has been reported [23], however the stability of these two compounds in fish are not known.

2.5. Software package ZebRA

A novel software package, named ZebRA, for automatically and accurately segmenting and quantifying the fluorescing yolk in images captured at the end of the treatment period was developed and can be downloaded from http://cbl.uh.edu/ZEBRAFISH/research/software/. The image processing algorithm of the software program was implemented in MATLAB 2012a with the Image Processing Toolbox. It consists of several steps, which are described in detail in the Supplementary Methods Text S1. The accuracy of the image processing algorithm was evaluated by computing the Dice similarity coefficient [24] between the segmented regions provided by the automated image processing algorithm of the software package and those provided by manual annotations. The Dice similarity coefficient is a spatial overlap measure, defined as:

$$\mathrm{DSC}(A, B) = 2\frac{|A \cap B|}{|A| + |B|} \quad (1)$$

where A and B denote two regions, $|A|$ and $|B|$ denote the corresponding areas, and $|A \cap B|$ denotes the area of the shared region. A value of the Dice similarity coefficient = 0 indicates no overlap between A and B regions while a value of 1 indicates total overlap. The manual annotations were performed by two authors who used a manual annotation tool (also developed in MATLAB 2012a), which is included in the software package. A detailed description of the evaluation is provided in the Supplementary Methods Text S2. The graphical user interface of the software program was developed in C++/Qt. As a result, the software program can be executed on computers running recent versions of Microsoft Windows. Furthermore, it has been designed to run the image processing algorithm on large sets of images at once. This allows quantitative results within hours of taking the images. The graphical user interface is described in the Supplementary Methods Text S3.

2.6. Statistical analyses

After image analysis, y_a ratios were computed using Microsoft Excel from Microsoft Office Professional Plus 2010. We define the y_a ratio as the ratio of the area of the yolk of the treated larva (measured in number of pixels) to the average yolk area of the respective control group of vehicle treated-larvae. One-way ANOVA with post-hoc Dunnett's test was performed using GraphPad Prism version 5.00 for Windows (GraphPad Software, San Diego, California USA). All treatment groups were compared to the DMSO-treated control group for Dunnett's analyses for statistical significance. GraphPad Prism version 5.00 was also used to prepare graphical representations. Vertical box and whiskers plots represent the distribution of y_a ratios across doses. The box extends from the 25th to 75th percentile, with the median (the line within the box) and the mean (+) represented. The whiskers run from 10th to 90th percentile of data points. For a given chemical, the stacked column graphs are representations of the same data values as those used to plot the box and whiskers graphs. GraphPad Prism version 5.00 was also used to plot zebrafish lethality dose curves and calculate LC_{50} values.

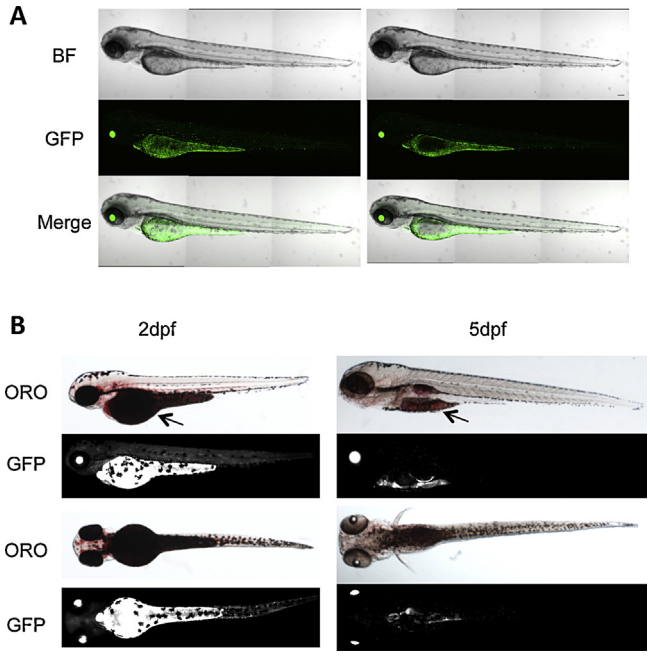

Fig. 1. Zebrafish as a model to investigate yolk malabsorption. (A) Images from confocal microscopy depicting a 3 dpf HGn50D larva expressing GFP in the yolk syncytial layer, the heart and the eye lens, as viewed using different channels (bright field or GFP). Left panel: Z projection of 46 slices (5 μm/slice) shows GFP expression in the aforementioned tissues/organs. Right panel: Z projection over 26 slices (5 μm/slice) shows that GFP expression is restricted to the yolk syncytial layer surrounding the yolk mass. Scale bar on the top right panel indicates 90 μm in length. (B) Oil Red O stained and GFP-fluorescent larvae at 2 and 5 dpf. For each time point, the top panel depicts the lateral view, and the bottom panel depicts the ventral view. The yolk (indicated by arrows) is rapidly used up between 2 and 5 dpf. These time points, 2 and 5 dpf, are depicted to represent the larvae at the beginning and end of the treatment period, respectively.

3. Results

3.1. GFP is expressed in the zebrafish yolk syncytial layer in the transgenic HGn50D line

To investigate yolk utilization in zebrafish embryos, we utilized the transgenic zebrafish line HGn50D. This transgenic line was generated by *Tol2*-mediated transposition and random insertion of the GFP expressing construct [17,18]. HGn50D embryos express GFP in the yolk, the eye lens, and the heart. The GFP of the yolk is expressed in the yolk syncytial layer as shown by confocal microscopy scanning through the yolk (Fig. 1A). The size of the yolk determined by GFP expression of live embryos can be correlated to that determined by Oil Red O staining of fixed fish at the same time points when imaged either ventrally or laterally (Fig. 1B).

3.2. Automated quantification of yolk size using ZebRA software package

To develop a high throughput screening method capturing the dynamics of yolk utilization of live fish, we utilized the HGn50D transgenic line. We imaged live fish at 5 dpf from the ventral side by fluorescence microscopy, which was minimally invasive for the fish and did not require any mounting of the fish as lateral imaging would have. The acquired images depicted the fish's yolk, heart, and eyes with higher fluorescent intensity than the rest of the fish.

To facilitate quantification of chemicals' effects on yolk absorption, we developed an automated image processing algorithm for the segmentation and quantification of the yolk (Supplementary Methods Text S1). First, the image was rotated so that the fish was

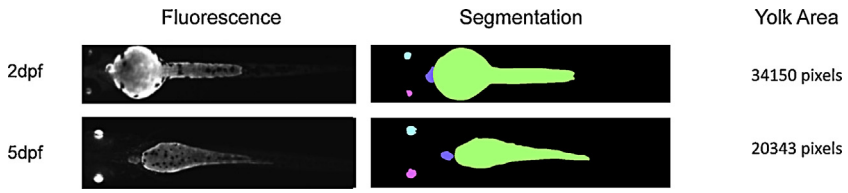

Fig. 2. Automatic segmentation and quantification of yolk area. Left panel: Images of 2 and 5 dpf larvae obtained on an Olympus IX51 inverted fluorescence microscope were cropped and oriented using the algorithm developed. Right panel: The processed images were automatically segmented. Representative output images depict the yolk in green, the heart in purple, and the eyes in pink and blue. Values indicate the number of pixels in the annotated yolk, as quantified by the algorithm. (For interpretation of the references to color in figure legend, the reader is referred to the web version of the article.)

depicted in horizontal orientation and was cropped so that only the fish and its immediate vicinity remained in a small rectangular image. Once the fish was depicted horizontally in the image, an iterative procedure was performed as follows: first, the brightness of the image was increased based on an intensity transformation. Subsequently, the image was segmented based on a thresholding technique and the connected components corresponding to the yolk, eyes and heart were identified. During the iterations the intensity transformation was changing. The iterations continued until the size of the connected component corresponding to the yolk area remained constant. Ultimately, the algorithm produced an image of the fish with each anatomical feature highlighted, along with the area (in pixels) of each feature (Fig. 2).

The accuracy of the image analysis algorithm was evaluated by computing the Dice similarity coefficient between the segmented regions provided by the automated image processing algorithm of the software package and the manual annotations. A manual annotation tool was developed in MATLAB to help validate the accuracy of the automated segmentation algorithm (Supplemental Methods Text S2). Using this tool, the user could open an image which was displaying a horizontally oriented fish as described above, and click on points around the edges of each yolk, heart, and eyes. Then, a curve was interpolated using those points and was filled in to show the shapes of each region. As a result, the anatomical regions of the yolk, heart and eyes were segmented and depicted with different colors. A reference set of images was selected that contained images with a variety of distinguishing qualitative characteristics (e.g., yolks with low intensity fluorescence, narrow-shaped yolks, small eyes, etc). Two of the authors used the manual annotation tool on the reference set, and their annotations were compared to the segmentation results of the automated algorithm. The similarity between the manual annotations and the automated segmentations was quantified by Dice's similarity coefficient [25]. Of the 320 images annotated manually, 309 (96.6%) were successfully segmented by the automated algorithm. The average Dice similarity coefficient was 0.932, with a standard deviation of 0.0476.

3.3. Screening of chemicals for effects on yolk utilization

After establishment of the quantitative assay for screening of chemicals affecting yolk utilization, we exposed zebrafish larvae from 2 to 5 dpf to a set of chemicals. Prochloraz, a chemical previously shown to cause yolk malabsorption, was selected as a positive control. We then tested two pharmaceuticals, clofibrate and gemfibrozil, two flame retardants, tetrabromobisphenol-A (TBBPA) and tetrachlorobisphenol-A (TCBPA), the biocide tributyltin (TBT), the surfactant perfluorooctanoic acid (PFOA), and two pesticides, imazalil and butralin. The embryos were treated in 6-well plates, allowing for unrestricted embryo motility. At the end of the treatment period, larvae were transferred into 96-well plates (1 larva/well) for imaging. Images were fed into the segmentation algorithm for processing and analysis. Next, the computed yolk area for each larva was used to calculate a "y_a ratio", defined as the ratio of the area of the yolk of the treated larva (measured in number of pixels) to the average yolk area of the control group of vehicle treated-larvae.

Prochloraz treatment from fertilization to 5 dpf has been shown previously to cause yolk malabsorption at 1.2 mg/L (approx. 3.18 μM) [14]. To validate our model and assay, we treated the HGn50D transgenic fish with different concentrations of prochloraz. In line with the previous study, treatment with prochloraz resulted in a significant delay in yolk absorption (Fig. 3A). Larvae treated with 100 nM, 1 μM and 10 μM of the prochloraz displayed significantly larger yolk sizes than those of the vehicle-treated control group. Larvae treated with 10 μM prochloraz suffered a severe malabsorption phenotype, causing most of the larvae to remain on their lateral sides, making imaging difficult. We also analyzed the proportion of larvae that exhibited a larger yolk size than the control group, and found that even at the lowest concentration tested (10 nM), slower yolk uptake was observed for around 60% of the embryos (Fig. 3B). We measured the dissolved oxygen levels in the E3 of untreated and prochloraz treated larvae at the end of the exposure period, and in E3 incubated without larvae. The levels of dissolved oxygen in the different samples ranged between 6.9 and 7.3 mg/L, which is well above the required oxygen levels for zebrafish maintenance (6 mg/L) [26]. These results indicate that the reduction in yolk absorption induced by prochloraz treatment is not caused by reduced oxygen levels in E3.

In zebrafish, the blood lipid lowering pharmaceuticals clofibrate and gemfibrozil have been shown to cause an embryonic malabsorption syndrome. Larvae treated with 0.5 and 0.75 mg/L (approx. 2 μM and 3 μM) clofibrate, and 5 mg/L (approx. 20 μM) gemfibrozil during early development display larger yolk sizes than vehicle-treated larvae [15]. While our experiments showed that there were no significant changes in yolk sizes after exposure to gemfibrozil (Fig. 3E) at 1 nM, 10 nM and 100 nM concentrations, clofibrate-treated larvae exhibited smaller yolk sizes compared to vehicle-treated larvae at 100 nM (Fig. 3C and D).

TBT, an antifouling agent used in paints in the shipping industry, and the flame retardants TBBPA and TCBPA have been shown to act as obesogens in the zebrafish [22,27]. We investigated whether these environmental obesogens, which induce lipid accumulation in 11 dpf zebrafish at 1 μM concentration for TBBPA and TCBPA and 1 nM for TBT, could cause abnormal mobilization of the lipid-rich yolk. In our assay, TBBPA and TCBPA, and TBT at 1 nM induced faster uptake of the yolk, with treated 5 dpf-larvae possessing smaller y_a ratios than those in the vehicle-treated control group (Fig. 4). Exposure to 10 and 100 pM TBT resulted in decreased yolk absorption.

We also treated the larvae with PFOA, a persistent organic pollutant with many industrial applications. In zebrafish, PFOA toxicity has been suggested to be mediated by mitochondrial dysfunction, causing an "energy drain" [28]. When treated with PFOA at 10 nM, 100 nM or 1 μM, there was no significant effect on the y_a ratio (Fig. 5A). However, approximately 60% of the larvae treated with 1 μM PFOA exhibited y_a ratios less than 1 (data not shown), indicating that a stronger effect could be possibly seen at higher doses.

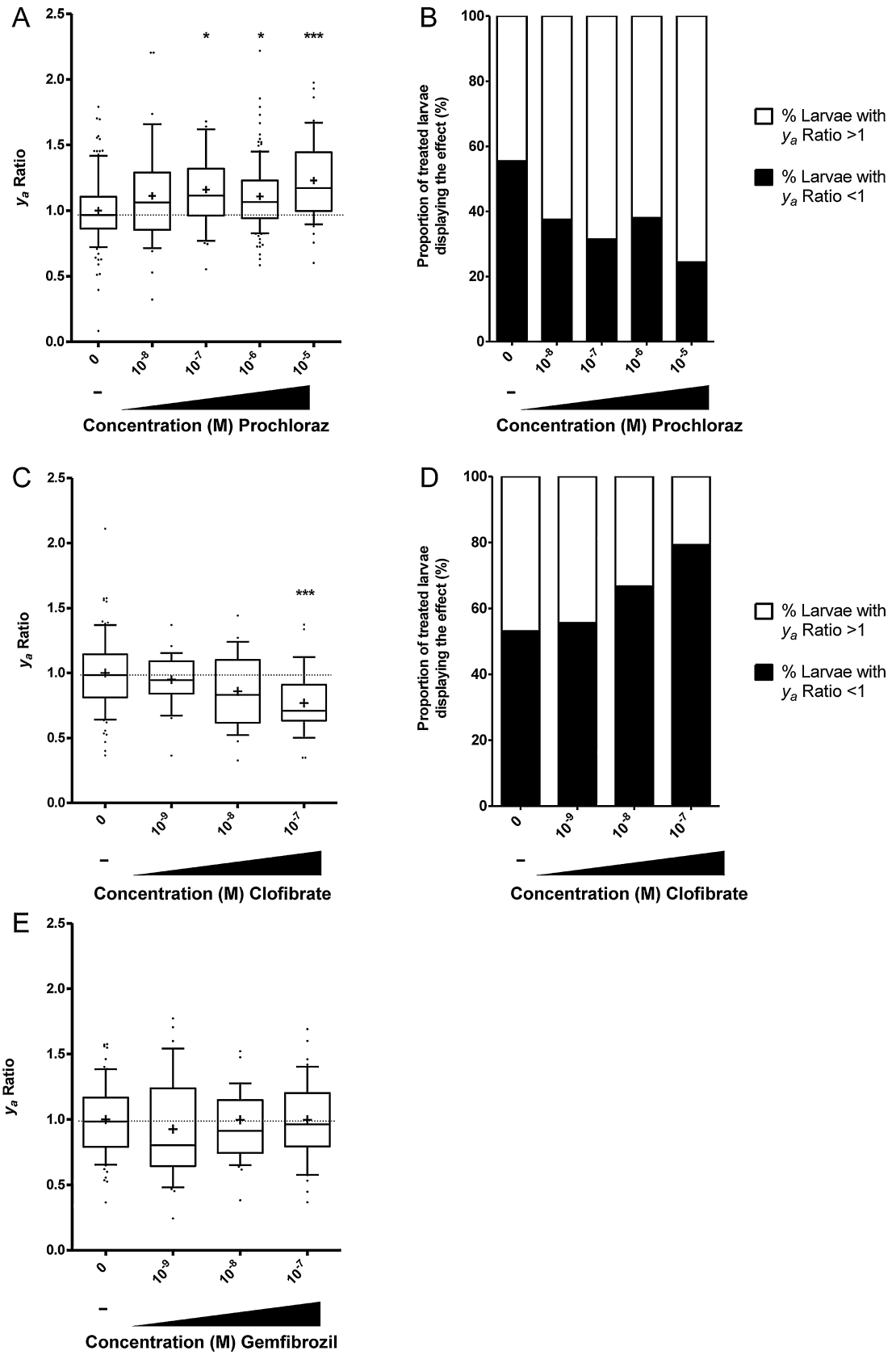

Fig. 3. Effect of prochloraz, clofibrate and gemfibrozil on yolk resorption. (A) Boxplot of the y_a ratios of prochloraz-treated larvae. (B) Stacked-column representation of the proportion of larvae within each prochloraz treatment group with y_a ratios less than or greater than 1. (C) Boxplot of y_a ratios of clofibrate-treated larvae. (D) Stacked-column representation of the proportion of larvae within each clofibrate treatment group with y_a ratios less than or greater than 1. (E) Boxplot of the mean of y_a ratios of gemfibrozil-treated larvae. Statistical evaluation was performed using one-way ANOVA. Asterisks indicate p values from a post-hoc Dunnett's Multiple Comparison test between each dose and the vehicle-treated group, with * indicating $p < 0.05$, and *** indicating $p < 0.001$.

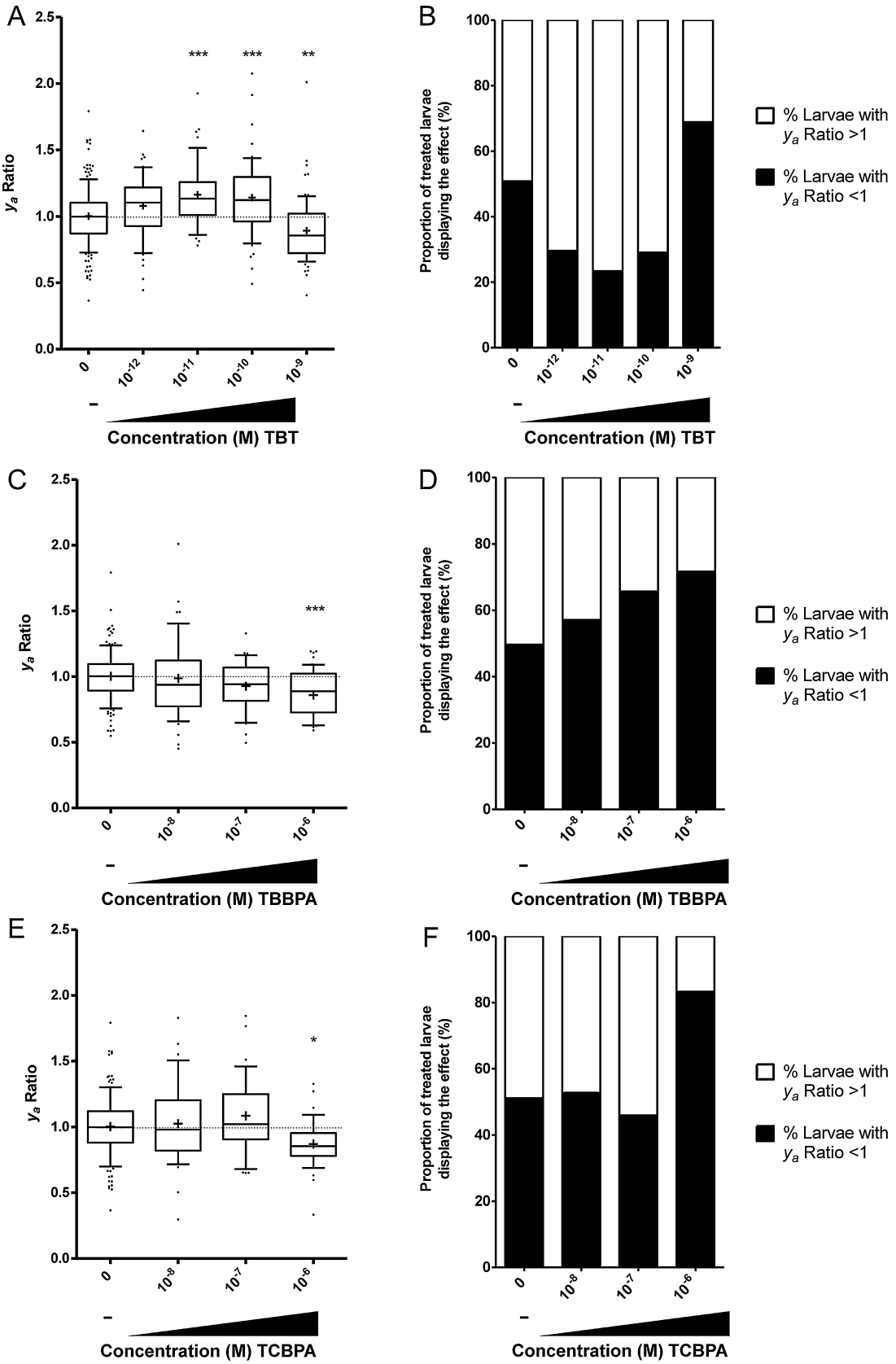

Fig. 4. Effects of obesogens on yolk resorption. Box plots of y_a ratios against different concentrations of TBT (A), TBBPA (C) and TCBPA (E). Stacked-column representation of the proportion of larvae within each treatment group with y_a ratios less than or greater than 1 for TBT (B), TBBPA (D) and TCBPA (E) respectively. Statistical evaluation was performed using one-way ANOVA. Asterisks indicate p values from a post-hoc Dunnett's Multiple Comparison test between each dose and the vehicle-treated group, with * indicating $p < 0.05$, ** indicating $p < 0.01$ and *** indicating $p < 0.001$.

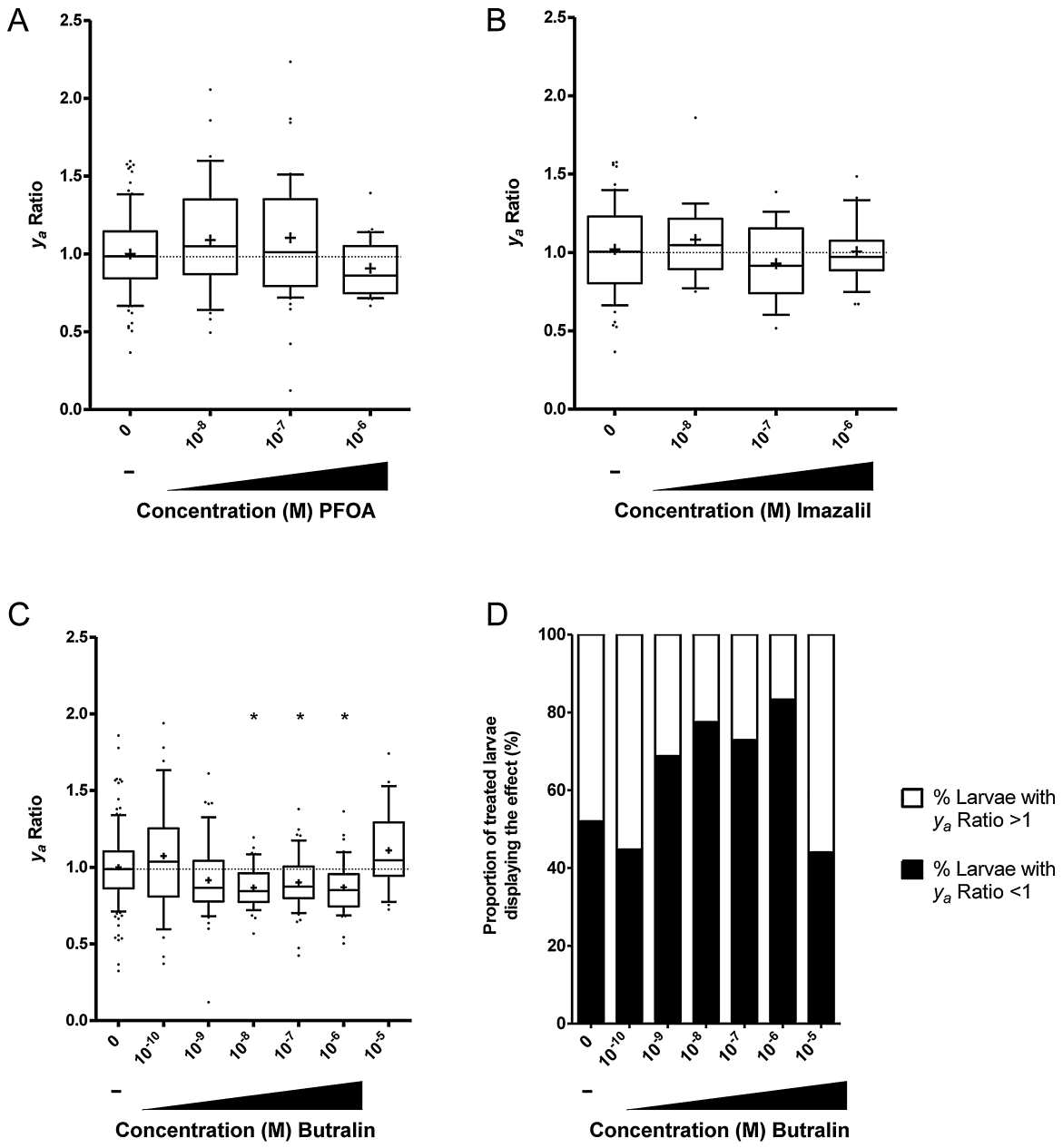

Fig. 5. Effect of endocrine disruptor PFOA and pesticides on yolk resorption. Box plots of y_a ratios against treatment concentration for PFOA (A), imazalil (B) and butralin (C). (D) Stacked-column representation of the proportion of larvae within each treatment group with y_a ratios less than or greater than 1 for butralin. Statistical evaluation was performed using one-way ANOVA. Asterisks indicate p values from a post-hoc Dunnett's Multiple Comparison test between each dose and the vehicle-treated group, with * indicating $p < 0.05$.

Finally, we exposed the embryos to the pesticides imazalil (a fungicide) and butralin (a herbicide). No significant effects were observed with imazalil (Fig. 5B). Larvae treated with 10 nM, 100 nM and 1 μM butralin displayed significantly smaller y_a ratios, implying faster consumption of the yolk than larvae in the control group (Fig. 5C). More than 70% of larvae treated with 10 nM, 100 nM or 1 μM butralin displayed a reduced yolk area compared to controls (Fig. 5D).

We also determined the LC50 of the chemicals, and their capacity to induce morphological malformations. Table 1 summarizes the chemicals' effects on yolk absorption measured as Lowest Observed Effect Concentration (LOEC) and the concentration required to cause 50% lethality (LC_{50}). An effect ratio was calculated by dividing the LC50 with the LOEC. By the LOEC the compound ranking from largest to lowest effect on yolk absorption is TBT > butralin > prochloraz, clofibrate > TBBPA, TCBPA. No significant morphological malformations other than altered yolk sizes were observed at the concentrations tested.

4. Discussion

In this study, we have designed and optimized a high-throughput zebrafish-based screening assay for yolk malabsorption. Environmental chemicals that alter the availability of nutrients to embryos during their development, across different species, can have important consequences for organogenesis, and also affect long-term risk of disease onset (reviewed in [29]). Given the number and variety of industrial chemicals in commerce today, the need for developing large-scale screening models to identify such chemicals is evident.

We used the transgenic line HGn50D, which fluoresces in the yolk syncytial layer, heart, and eye lens. HGn50D was generated

Table 1
LC50, LEL, and effect and y_a ratio for test chemicals.

Chemical	LC50 (M)	LEL (M)	Effect ratio (LC50/LEL)	Median y_a ratio at the LEL
Prochloraz	3.6×10^{-5}	1×10^{-7}	360	1.11
Clofibrate	3.1×10^{-7}	None	NA	NA
Gemfibrozil	3.4×10^{-6}	None	NA	NA
TBT	3.4×10^{-7}	1×10^{-11}	34,400	1.13
TBBPA	3.6×10^{-6}	1×10^{-6}	3.6	0.89
TCBPA	3.6×10^{-6}	1×10^{-6}	3.6	0.85
PFOA	3.8×10^{-4}	None	NA	NA
Imazalil	6.6×10^{-5}	None	NA	NA
Butralin	9.5×10^{-5}	1×10^{-8}	9500	0.84

by *Tol2*-mediated transposition and random insertion of the GFP expressing construct [17,18], and the promoter driving the expression of GFP in the transgenic line is not known. Therefore, we have not considered the intensity of the fluorescence in yolk syncytial layer, and have only quantified the area within boundaries of the fluorescing yolk syncytial layer after chemical exposures. The effects of the chemicals on the other fluorescing tissues (heart and eyes) have not been assessed here.

MATLAB was used for development of the automated image processing algorithm. The existence and widespread use of the Image Processing Toolbox for MATLAB simplified the implementation of the complex algebra required to process the images. Several generalized algorithms for image processing have been developed, but the need to identify specific regions of zebrafish in images with a variety of artifacts, and containing fish exhibiting highly diverse yolk morphology led to the need for an *ad hoc* algorithm to annotate and quantify the yolk.

There were several complications in developing the image processing algorithm of the ZebRA software package. As the larvae were imaged live and free-swimming, they were localized at an arbitrary orientation and position in the image. This initially required manually rotating the image to orient the fish correctly using ImageJ, followed by cropping to shrink the image to contain only the fish. The manual orientation process was accelerated through the automated rotation and cropping of the image. Other issues included artifacts of the walls of the plate used to contain the fish during microscopy appearing on the image, which was resolved by removing large features on the edges of the images. The fact that some fish had pigmentation within the yolk exterior occasionally caused the fluorescence of the yolk to appear split into two or more distinct regions; this issue was resolved by vertically connecting these separated regions and assuming that all pixels between the two or more regions were also part of the yolk. The algorithm was developed to quantify the yolk size of fluorescent zebrafish imaged ventrally and pixels were used to measure yolk size. As a result magnification and image resolution were required to be held constant across all images that were compared with each other. Should these parameters be changed, two images could still be compared by extrapolating the yolk sizes, providing the magnifications and resolutions are known.

Chemical exposures in our studies were restricted to 2–5 dpf. We chose the 2 dpf time point because this is after most organ rudiments have developed. An earlier exposure window might lead to developmental perturbations that could indirectly affect yolk absorption. We tested a dose range of exposures for all the chemicals. The low doses tested allowed for identification of yolk malabsorption in larvae that otherwise appeared normal morphologically, suggesting that chemicals, which impacted yolk absorption in our studies, can have effects at low doses even if there are no other observable gross morphological abnormalities. These results, therefore, underline the need for toxicological testing to assess less obvious endpoints at low doses.

Using our novel method, we first confirmed that prochloraz induces yolk malabsorption. Prochloraz is an imidazole fungicide used widely in Europe, Australia, Asia and South America, in both agricultural and gardening practices. It acts as an endocrine disruptor via multiple modes of action. *In vitro*, it antagonizes the androgen and estrogen receptors, inhibits aromatase and activates the aryl hydrocarbon receptor [30–33]. *In vivo*, prochloraz acts as an anti-androgen in adult and developmental stages in rodents [34,35]. In zebrafish, prochloraz exposure causes metabolic alterations in exposed zebrafish larvae [14], which is in line with our results, and in adults [36]. Spine malformation, pericardial edema and yolk malabsorption are observed when embryos/larvae are treated from 0 to 3 or 0 to 4 dpf, at concentrations of 1.2 mg/L (approx. 3.18 μM) or higher [14]. However, in our studies, we observed a significant yolk malabsorption effect at lower concentrations (as low as 100 nM), possibly reflecting the high sensitivity of our quantification method.

The pharmaceutical fibrates clofibrate and gemfibrozil have previously been suggested to induce yolk malabsorption, albeit at concentrations higher than tested here. For clofibrate, Raldua et al. [15] showed that yolk malabsorption occurred at 0.75–1.00 mg/L (approx. 3–4 μM), with affected embryos displaying a larger yolk than control embryos. However, at the highest concentration we tested (100 nM), treated larvae have significantly smaller yolk sizes than vehicle-treated larvae, with more than 75% of the embryos displaying a y_a ratio less than 1. This result highlights the importance of testing low concentrations using sensitive and quantitative endpoints. Raldua et al. [15] also showed that gemfibrozil at 5 mg/L (approx. 20 μM) caused yolk malabsorption. In our study, however, we did not observe significant changes in yolk absorption at low concentrations of gemfibrozil (1 nM, 10 nM and 100 nM), and the larvae did not survive in concentrations of 1 μM or higher. It is worth noting here, that there were important differences in our experimental design. We treated the fish only from 2 dpf, and not from 4 h post fertilization (hpf), and only with lower concentrations of the chemicals. This might explain why we did not see drastic effects, as it is possible that these chemicals induce a stronger effect earlier during development. Mortality at 1 μM concentrations may be due to the fact that we did not replace the treatment solutions each day of the treatment. It is possible that accumulation of toxic metabolites of these chemicals were highly toxic to the larvae.

Using our assay, we observed an increased uptake of the yolk in larvae treated with the flame retardants TBBPA and TCBPA, and with TBT, an antifouling agent used in paints in the shipping industry. These compounds have been suggested to be obesogens, environmental chemicals that can cause obesity. Given the steep rise in obesity prevalence in recent years [37,38], the putative role of chemicals in inducing obesity is an active area of research (reviewed in [39]). TBT induces adipogenesis *in vitro* [40,41] and causes obesity or lipid accumulation *in vivo*, in mice [42] and in zebrafish [22,27]. Recent studies by us and others have shown that TBBPA and TCBPA can act as obesogens *in vitro* [43] and *in vivo* in zebrafish [22]. TBBPA and TCBPA are ligands for the zebrafish peroxisome proliferator-activated receptor gamma (PPARγ) [22]. Whether or not PPARγ is involved in yolk absorption, however, is not known. Larvae treated with PFOA, an endocrine disruptor [44] and a chemical associated with mitochondrial dysfunction in zebrafish [28], did not show significant effects on yolk utilization in our study (Fig. 5A). However, approximately 60% of 1 μM treated larvae displayed smaller yolk sizes as compared to controls (data not shown), indicating that perhaps a stronger effect can be seen at higher doses. As our assay was able to detect the altered yolk consumption rates of known disruptors of energy/lipid metabolism, we suggest that our assay may be used to supplement other screening efforts designed to identify chemicals altering metabolic endpoints.

We also analyzed the effects of two pesticides from the ToxCast phase I chemical library, imazalil, and butralin, on yolk absorption. Imazalil, which is a fungicide and food contaminant, is known to induce cytochrome P450 isoforms in the mouse intestine [45], and alter developmental endpoints, including cardiac edema, and deformations in the notochord and tail in the zebrafish [46]. In our experiments, we did not see significant effects of imazalil, possibly because of the low concentrations tested. Butralin, on the other hand, significantly increased yolk uptake, with y_a ratios across four different concentrations being less than the average of the control group. Butralin, a dinitroaniline compound, is an herbicide used on agricultural crops, including tobacco. Very little is known about its potential other biological effects. In a retrospective epidemiological study conducted on tobacco farmers, exposure to the pesticide Tamex, containing butralin, was found to significantly correlate to low maximal motor nerve conduction velocity, indicating a possible effect on the nervous system [47]. As little is known about the chemical's mechanism of toxicity, it is not possible to speculate on how butralin causes yolk malabsorption, although its potential effects on the nervous system could be worth investigating.

In conclusion, we have established an assay for the quantification of the yolk size in zebrafish larvae exposed to different environmental chemicals and showed that several chemicals alter yolk absorption. Although elucidation of the mechanisms through which the chemicals impacting our assay elicit their effect on yolk absorption is beyond the scope of this study, it would be interesting to differentiate a chemical's effect on the chosen endpoint as being a direct or an indirect effect. It will also be interesting to investigate long-term effects of the chemicals that disturb nutritional balance during zebrafish development. Moreover, chemicals causing alterations in this assay could be tested on other animal models to ascertain their relevance, perhaps, in a mammalian context.

Funding

This study was funded by grants from the Environmental Protection Agency (R834289), the National Institute of Health/National Institute of Environmental Health Sciences (R21ES020036), and in part by a training fellowship from the Keck Center Computational Cancer Biology Training Program of the Gulf Coast Consortia (CPRIT Grant No. RP101489). JÅG is grateful for a grant from the Robert A. Welch Foundation (E-0004). The views expressed in the article do not necessarily reflect the views of the funders.

Conflict of interest

The authors declare that there are no conflicts of interest.

Transparency document

The Transparency document associated with this article can be found in the online version.

Acknowledgements

We would like to thank Dr. Kawakami, the National BioResource Project from the Ministry of Education, Culture, Sports, Science and Technology of Japan for the transgenic fish HGn50D.

Appendix A. Supplementary data

Supplementary data associated with this article can be found, in the online version, at http://dx.doi.org/10.1016/j.reprotox.2014.10.022.

References

[1] Wu G, Bazer FW, Wallace JM, Spencer TE. Board-invited review: intrauterine growth retardation: implications for the animal sciences. J Anim Sci 2006;84:2316–37.
[2] McMillen IC, MacLaughlin SM, Muhlhausler BS, Gentili S, Duffield JL, Morrison JL. Developmental origins of adult health and disease: the role of periconceptional and foetal nutrition. Basic Clin Pharmacol Toxicol 2008;102:82–9.
[3] Parke DV, Ioannides C. The role of nutrition in toxicology. Annu Rev Nutr 1981;1:207–34.
[4] Hennig B, Toborek M, Bachas LG, Suk WA. Emerging issues: nutritional awareness in environmental toxicology. J Nutr Biochem 2004;15:194–5.
[5] Hennig B, Reiterer G, Majkova Z, Oesterling E, Meerarani P, Toborek M. Modification of environmental toxicity by nutrients: implications in atherosclerosis. Cardiovasc Toxicol 2005;5:153–60.
[6] Wiegand MD. Composition accumulation and utilization of yolk lipids in teleost fish. Rev Fish Biol Fish 1996;6:259–86.
[7] Ng AN, de Jong-Curtain TA, Mawdsley DJ, White SJ, Shin J, Appel B, et al. Formation of the digestive system in zebrafish: III. Intestinal epithelium morphogenesis. Dev Biol 2005;286:114–35.
[8] Poupard G, Andre M, Durliat M, Ballagny C, Boeuf G, Babin PJ. Apolipoprotein E gene expression correlates with endogenous lipid nutrition and yolk syncytial layer lipoprotein synthesis during fish development. Cell Tissue Res 2000;300:251–61.
[9] Carvalho L, Heisenberg CP. The yolk syncytial layer in early zebrafish development. Trends Cell Biol 2010;20:586–92.
[10] Donovan A, Brownlie A, Zhou Y, Shepard J, Pratt SJ, Moynihan J, et al. Positional cloning of zebrafish ferroportin1 identifies a conserved vertebrate iron exporter. Nature 2000;403:776–81.
[11] Hsu HJ, Lin JC, Chung BC. Zebrafish cyp11a1 and hsd3b genes: structure, expression and steroidogenic development during embryogenesis. Mol Cell Endocrinol 2009;312:31–4.
[12] Mudumana SP, Wan H, Singh M, Korzh V, Gong Z. Expression analyses of zebrafish transferrin, ifabp, and elastaseB mRNAs as differentiation markers for the three major endodermal organs: liver, intestine, and exocrine pancreas. Dev Dyn 2004;230:165–73.
[13] Schlegel A, Stainier DY. Microsomal triglyceride transfer protein is required for yolk lipid utilization and absorption of dietary lipids in zebrafish larvae. Biochemistry 2006;45:15179–87.
[14] Domingues I, Oliveira R, Musso C, Cardoso M, Soares AM, Loureiro S. Prochloraz effects on biomarkers activity in zebrafish early life stages and adults. Environ Toxicol 2013;28:155–63.
[15] Raldua D, Andre M, Babin PJ. Clofibrate and gemfibrozil induce an embryonic malabsorption syndrome in zebrafish. Toxicol Appl Pharmacol 2008;228:301–14.
[16] Kimmel CB, Ballard WW, Kimmel SR, Ullmann B, Schilling TF. Stages of embryonic development of the zebrafish. Dev Dyn 1995;203:253–310.
[17] Urasaki A, Asakawa K, Kawakami K. Efficient transposition of the Tol2 transposable element from a single-copy donor in zebrafish. Proc Natl Acad Sci U S A 2008;105:19827–32.
[18] Asakawa K, Suster ML, Mizusawa K, Nagayoshi S, Kotani T, Urasaki A, et al. Genetic dissection of neural circuits by Tol2 transposon-mediated Gal4 gene and enhancer trapping in zebrafish. Proc Natl Acad Sci U S A 2008;105:1255–60.
[19] Aktar MW, Sengupta D, Purkait S, Ganguly M, Paramasivam M. Degradation dynamics and dissipation kinetics of an imidazole fungicide (Prochloraz) in aqueous medium of varying pH. Interdiscip Toxicol 2008;1:203–5.
[20] Food and Agriculture Organization of the United Nations. Pesticide residues in food. In: 1977, report of the joint meeting of the FAO panel of experts on pesticide residues and environment and the WHO expert committee on pesticide residues held in Geneva, 6–15 December 1977 FAO plant production and protection paper; 10 Rev1978. 1977.
[21] Vierke L, Staude C, Biegel-Engler A, Drost W, Schulte C. Perfluorooctanoic acid (PFOA)—main concerns and regulatory developments in Europe from an environmental point of view. Environ Sci Eur 2012;24:1–11.
[22] Riu A, McCollum CW, Pinto CL, Grimaldi M, Hillenweck A, Perdu E, et al. Halogenated bisphenol-A analogs act as obesogens in zebrafish larvae (*Danio rerio*). Toxicol Sci 2014;39:48–58.
[23] Brox S, Ritter AP, Kuster E, Reemtsma T. A quantitative HPLC-MS/MS method for studying internal concentrations and toxicokinetics of 34 polar analytes in zebrafish (*Danio rerio*) embryos. Anal Bioanal Chem 2014;406:4831–40.
[24] Dice LR. Measures of the amount of ecologic association between species. Ecology 1945;26:297–302.
[25] Zou KH, Warfield SK, Bharatha A, Tempany CM, Kaus MR, Haker SJ, et al. Statistical validation of image segmentation quality based on a spatial overlap index. Acad Radiol 2004;11:178–89.
[26] Avdesh A, Chen M, Martin-Iverson MT, Mondal A, Ong D, Rainey-Smith S, et al. Regular care and maintenance of a zebrafish (*Danio rerio*) laboratory: an introduction. J Vis Exp 2012:e4196.
[27] Tingaud-Sequeira A, Ouadah N, Babin PJ. Zebrafish obesogenic test: a tool for screening molecules that target adiposity. J Lipid Res 2011;52:1765–72.
[28] Hagenaars A, Vergauwen L, Benoot D, Laukens K, Knapen D. Mechanistic toxicity study of perfluorooctanoic acid in zebrafish suggests mitochondrial dysfunction to play a key role in PFOA toxicity. Chemosphere 2013;91:844–56.

[29] Gluckman PD, Hanson MA, Beedle AS. Early life events and their consequences for later disease: a life history and evolutionary perspective. Am J Hum Biol 2007;19:1–19.
[30] Andersen HR, Vinggaard AM, Rasmussen TH, Gjermandsen IM, Bonefeld-Jorgensen EC. Effects of currently used pesticides in assays for estrogenicity, androgenicity, and aromatase activity in vitro. Toxicol Appl Pharmacol 2002;179:1–12.
[31] Laignelet L, Riviere JL, Lhuguenot JC. Metabolism of an imidazole fungicide (prochloraz) in the rat after oral administration. Food Chem Toxicol 1992;30:575–83.
[32] Long M, Laier P, Vinggaard AM, Andersen HR, Lynggaard J, Bonefeld-Jorgensen EC. Effects of currently used pesticides in the AhR-CALUX assay: comparison between the human TV101L and the rat H4IIE cell line. Toxicology 2003;194:77–93.
[33] Vinggaard AM, Hnida C, Breinholt V, Larsen JC. Screening of selected pesticides for inhibition of CYP19 aromatase activity in vitro. Toxicology In vitro 2000;14:227–34.
[34] Vinggaard AM, Nellemann C, Dalgaard M, Jorgensen EB, Andersen HR. Antiandrogenic effects in vitro and in vivo of the fungicide prochloraz. Toxicol Sci 2002;69:344–53.
[35] Vinggaard AM, Hass U, Dalgaard M, Andersen HR, Bonefeld-Jorgensen E, Christiansen S, et al. Prochloraz: an imidazole fungicide with multiple mechanisms of action. Int J Androl 2006;29:186–92.
[36] Biales AD, Bencic DC, Villeneuve DL, Ankley GT, Lattier DL. Proteomic analysis of zebrafish brain tissue following exposure to the pesticide prochloraz. Aquat Toxicol 2011;105:618–28.
[37] Ogden CL, Carroll MD, Kit BK, Flegal KM. Prevalence of obesity in the United States, 2009–2010. NCHS Data Brief 2012:1–8.
[38] Ogden CL, Carroll MD, Kit BK, Flegal KM. Prevalence of childhood and adult obesity in the United States, 2011–2012. JAMA 2014;311:806–14.
[39] Baillie-Hamilton PF. Chemical toxins: a hypothesis to explain the global obesity epidemic. J Altern Complement Med 2002;8:185–92.
[40] Inadera H, Shimomura A. Environmental chemical tributyltin augments adipocyte differentiation. Toxicol Lett 2005;159:226–34.
[41] Li X, Ycaza J, Blumberg B. The environmental obesogen tributyltin chloride acts via peroxisome proliferator activated receptor gamma to induce adipogenesis in murine 3T3-L1 preadipocytes. J Steroid Biochem Mol Biol 2011;127:9–15.
[42] Zuo Z, Chen S, Wu T, Zhang J, Su Y, Chen Y, et al. Tributyltin causes obesity and hepatic steatosis in male mice. Environ Toxicol 2011;26:79–85.
[43] Riu A, Grimaldi M, le Maire A, Bey G, Phillips K, Boulahtouf A, et al. Peroxisome proliferator-activated receptor gamma is a target for halogenated analogs of bisphenol A. Environ Health Perspect 2011;119:1227–32.
[44] Du G, Huang H, Hu J, Qin Y, Wu D, Song L, et al. Endocrine-related effects of perfluorooctanoic acid (PFOA) in zebrafish, H295R steroidogenesis and receptor reporter gene assays. Chemosphere 2013;91:1099–106.
[45] Muto N, Hirai H, Tanaka T, Itoh N, Tanaka K. Induction and inhibition of cytochrome P450 isoforms by imazalil, a food contaminant, in mouse small intestine and liver. Xenobiotica 1997;27:1215–23.
[46] Sisman T, Turkez H. Toxicologic evaluation of imazalil with particular reference to genotoxic and teratogenic potentials. Toxicol Ind Health 2010;26:641–8.
[47] Kimura K, Yokoyama K, Sato H, Nordin RB, Naing L, Kimura S, et al. Effects of pesticides on the peripheral and central nervous system in tobacco farmers in Malaysia: studies on peripheral nerve conduction, brain-evoked potentials and computerized posturography. Ind Health 2005;43:285–94.